
OpenOOD v1.5: Enhanced Benchmark for Out-of-Distribution Detection

Jingyang Zhang¹, Jingkang Yang², Pengyun Wang³, Haoqi Wang⁴,
Yueqian Lin⁵, Haoran Zhang¹, Yiyu Sun⁶, Xuefeng Du⁶, Kaiyang Zhou²,
Wayne Zhang⁴, Yixuan Li⁶, Ziwei Liu², Yiran Chen¹, Hai Li¹

¹Duke University, Durham, USA ²S-Lab, Nanyang Technological University, Singapore

³Beijing University of Posts and Telecommunications, Beijing, China

⁴SenseTime Research, Shenzhen, China ⁵Duke Kunshan University, Kunshan, China

⁶University of Wisconsin-Madison, Madison, USA

Code: <https://github.com/Jingkang50/OpenOOD/>

Leaderboard: <https://zjysteven.github.io/OpenOOD/>

Abstract

Out-of-Distribution (OOD) detection is critical for the reliable operation of open-world intelligent systems. Despite the emergence of an increasing number of OOD detection methods, the evaluation inconsistencies present challenges for tracking the progress in this field. OpenOOD v1 initiated the unification of the OOD detection evaluation but faced limitations in scalability and usability. In response, this paper presents OpenOOD v1.5, a significant improvement from its predecessor that ensures accurate, standardized, and user-friendly evaluation of OOD detection methodologies. Notably, OpenOOD v1.5 extends its evaluation capabilities to large-scale datasets such as ImageNet, investigates full-spectrum OOD detection which is important yet underexplored, and introduces new features including an online leaderboard and an easy-to-use evaluator. This work also contributes in-depth analysis and insights derived from comprehensive experimental results, thereby enriching the knowledge pool of OOD detection methodologies. With these enhancements, OpenOOD v1.5 aims to drive advancements and offer a more robust and comprehensive evaluation benchmark for OOD detection research.

1 Introduction

1.1 Background and Motivation

For intelligent recognition systems to operate reliably in the open world, it is crucial for them to have the capability of detecting and handling unknown inputs. This problem is commonly formulated as Out-of-Distribution (OOD) detection [1] or Open-Set Recognition (OSR) [2]. In the context of image classification, OOD detection seeks to enable the identification of images that do not belong to any of the known, in-distribution (ID) categories of the classifier.

Recent years have witnessed a surge of over a hundred papers on OOD detection [3]. Despite the increasing attention and the importance of this research problem, tracking the progress in the field has been hindered by several *evaluation pitfalls* that are often overlooked by researchers.

Confusing terminologies. Despite subtle differences in the way of constructing their test environments, OOD detection and OSR (or sometimes, “novelty detection”) are essentially pursuing the same goal [2, 1]. With two different terminologies, however, the two topics often diverge from each other in a counterproductive way, where methods are developed and compared separately within each branch using different benchmarks.

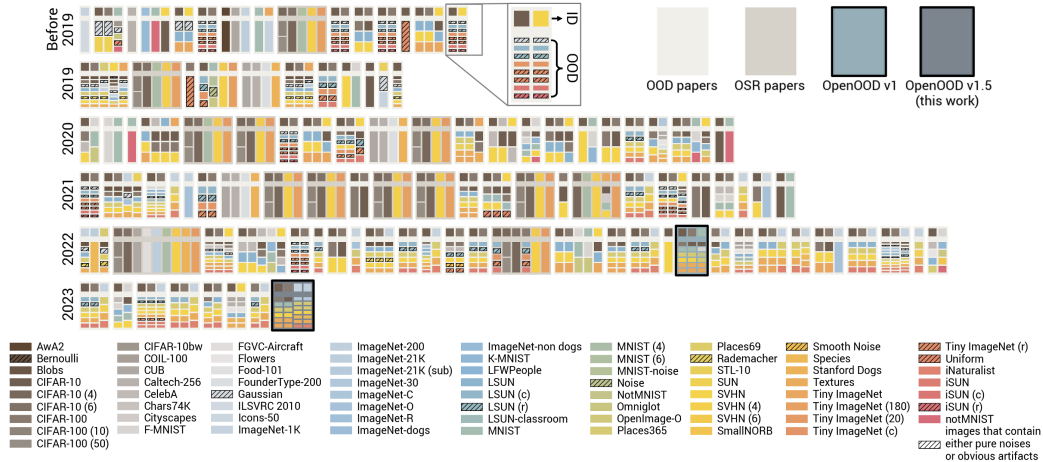


Figure 1: Summarizing evaluation settings of 100+ recent OOD detection and OSR works from NeurIPS, AAAI, ICLR, CVPR, ICML, and ICCV/ECCV (zoom in to view better). Each box stands for a paper. Within the box, each column shows the ID dataset and corresponding OOD datasets which are represented by the color blocks. The lack of a consistent color pattern between boxes signifies the inconsistency in the evaluation setup of current works. Multiple works also adopted unrealistic or problematic data [7] in evaluation (marked by the hatch pattern). The community still suffers from such chaos after OpenOOD v1 [8] came out. Full paper list used to produce this figure can be found [here](#).

Inconsistent datasets. Given an ID dataset, the simplest practice is to use other datasets with semantically different visual categories as OOD datasets. Unfortunately, we have seen great inconsistency in the selected datasets for OOD detection evaluation. Such phenomenon is highlighted in Figure 1, where we summarize the evaluation settings of 100+ recent works from top-tier machine learning conferences. The lack of a consistent pattern indicates how different the used datasets are from paper to paper, causing great difficulty for straight comparison between methods. The evaluation settings within the OSR branch are more consistent, despite being significantly limited in scale as we will discuss later.

Erroneous practices could compromise evaluation if no extra care is taken. One example that is pervasive in OOD detection works is leaking information about OOD data that is used for evaluation. More specifically, some methods train the model or tune hyperparameters with test OOD data [4, 5, 6]. Such practices go against basic machine learning principles and will lead to overoptimistic results.

Apparently, the OOD detection community has a pressing need for a unified test platform and benchmark for accurate evaluation of current and future methodologies. One work that comes close to this goal is the first version of OpenOOD [8], which implemented multiple methods within a curated framework and evaluated them using designed benchmarks. However, OpenOOD v1 has certain limitations in *scalability* and *usability*. Specifically, its evaluation was mostly performed on small-scale datasets like MNIST [9] and CIFAR [10, 11], while large-scale datasets such as ImageNet [12] carry greater importance and have received increasing attention recently [13, 14, 15, 16, 17, 18]. Meanwhile, OpenOOD v1 lacks certain features that ensure seamless use experience (*e.g.*, users have to go through a complex pipeline to evaluate their custom models or methods).

1.2 New Contributions of OpenOOD v1.5

Building upon OpenOOD v1, in this work we present OpenOOD v1.5 which aims to further enable easy, fair, and accurate evaluation of OOD detection. Concretely, we make the following extensions and contributions.

Large-scale experiments and results. In addition to the small datasets included in v1, OpenOOD v1.5 provide extensive experiment results for nearly 40 methods (and their combinations) on ImageNet-1K, which serve as a comprehensive reference for later works. To facilitate future research



Figure 2: **Left:** An example of evaluating ImageNet-1K models in a few lines with our Evaluator. **Right:** Screenshot of top entries on our ImageNet-1K leaderboard hosted at <https://zjysteven.github.io/OpenOOD/>. Zoom in to view better.

on large-scale settings with affordable computational cost, we also introduce a new benchmark constructed with ImageNet-200, a subset of ImageNet-1K.

Investigation on full-spectrum detection. Besides the *standard* setting considered in v1, OpenOOD v1.5 also closely studies *full-spectrum* OOD detection [19], an important setting that considers OOD *generalization* [20, 21] and OOD *detection* at the same time. Compared with the standard setting which is adopted by existing works, we show that full-spectrum detection poses significant challenge for all current approaches.

New insights. With comprehensive results from OpenOOD v1.5, we are able to provide several valuable observations. For example, we identify that there is *no single winner* that always outperforms others across multiple datasets. Meanwhile, we observe that *data augmentations* [22, 23, 24, 21, 25, 26] *help* with OOD detection in both standard and full-spectrum setting. Our insights help assess the current state of OOD detection and provide future directions for the community.

New features and updates. Lastly, OpenOOD v1.5 introduces new features including a *leaderboard* hosted online to track the-state-of-the-art based on various methods and a lightweight *evaluator* which enables easy evaluation with a few lines of code (see Figure 2). Other updates such as adding newer methods and fixing implementation bugs are documented in the [changelog](#).

2 Problem Statement and Evaluation Protocol

This work considers OOD detection in the context of (supervised) multi-class image classification. In this section, we formally describe the problem statement and present the evaluation protocol specified by OpenOOD for both *standard* and *full-spectrum* setting.

2.1 Standard OOD Detection

There are two goals in standard OOD detection. We first establish context. In each image classification problem, there exists a pre-defined set of semantic categories that we expect the model to identify (*e.g.*, `dog` and `automobile` in CIFAR-10), which defines what images are considered in-distribution (ID). We refer to the group of labels and the associated joint distribution as \mathcal{Y}_{ID} and \mathcal{D}_{ID} , respectively, where $\forall (x, y) \sim \mathcal{D}_{ID}, y \in \mathcal{Y}_{ID}$. In an open world, there exists semantic groups that don't belong to the pre-defined and finite \mathcal{Y}_{ID} , which forms the out-of-distribution (OOD) space $\mathcal{Y}_{OOD} = \{y | y \notin \mathcal{Y}_{ID}\}$ and \mathcal{D}_{OOD} .

Goal ① The first goal of OOD detection is to have a discriminative model that accurately classifies ID samples drawn from \mathcal{D}_{ID} . To evaluate this goal, we use widely adopted image classification datasets (such as CIFAR and ImageNet) as the target distribution \mathcal{D}_{ID} . As in normal classification tasks, we train the classifier with specific methods by minimizing the empirical risk on the training dataset \mathcal{D}_{ID}^{train} and evaluate its performance on the unseen ID test images \mathcal{D}_{ID}^{test} . The metric for goal ① is classification accuracy.

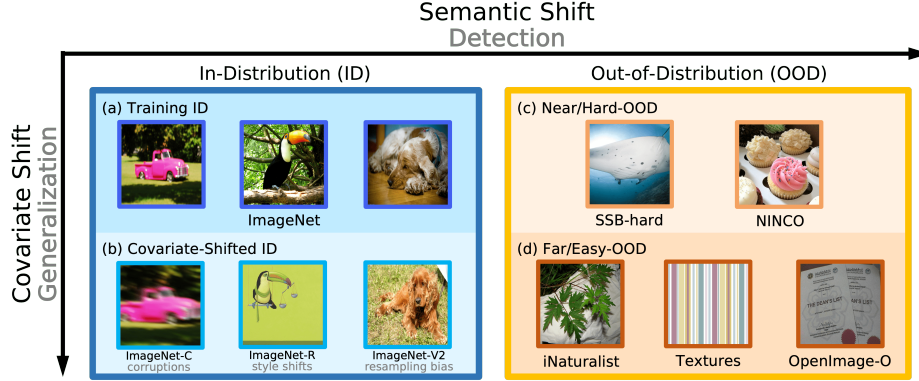


Figure 3: Illustration of full-spectrum OOD detection [29]. Standard detection only concerns *semantic* shift by detecting (c) + (d) from (a), while full-spectrum detection takes into account *covariate* shift and aims to separate (c) + (d) from (a) + (b). An ideal system should be robust to the non-semantic covariate shift (OOD *generalization*) while being able to identify semantic shift (OOD *detection*).

Goal ② The second goal is to have a detector module (typically built upon the trained classifier) that accurately identifies whether an incoming image in the inference phase is ID or OOD, *i.e.*, $y \in \mathcal{Y}_{ID}$ or $y \notin \mathcal{Y}_{ID}$. Following common practices, we take publicly available datasets whose categories are OOD w.r.t. \mathcal{Y}_{ID} as the source of OOD samples \mathcal{D}_{OOD} . Since certain methods incorporate OOD images at training time to improve OOD detection capability [27, 28, 29, 30], we make distinction between OOD training samples $\mathcal{D}_{OOD}^{train}$ and OOD test samples \mathcal{D}_{OOD}^{test} , where they should have non-overlapping categories between each other (*i.e.*, $\mathcal{Y}_{OOD}^{train} \cap \mathcal{Y}_{OOD}^{test} = \emptyset$) to avoid trivial evaluation [27]. For each ID test set \mathcal{D}_{ID}^{test} , we use multiple OOD test sets \mathcal{D}_{OOD}^{test} and measure the OOD detection performance on each ID-OOD pair. We treat OOD samples as *positive* and ID samples as *negative*. We use the well established 1) area under the receiver operating characteristic (AUROC), 2) area under the Precision-Recall curve (AUPR), and 3) false positive rate at 95% true negative rate (FPR@95) as metrics for goal ②. AUROC and AUPR are threshold-independent measurements, while FPR95 reflects the performance at a specific threshold.

Remark. *There are two extra efforts that make our evaluation protocol much more rigorous than prior works.* First, OpenOOD divides considered OOD datasets into two groups: near-OOD and far-OOD (or equivalently, hard-OOD and easy-OOD). The grouping is based on either image semantics or empirical difficulty, which can give a more comprehensive evaluation of OOD detectors in the face of different types of OOD samples (see Appendix A for details). Second, we introduce ID validation samples \mathcal{D}_{ID}^{val} and OOD validation samples \mathcal{D}_{OOD}^{val} in all evaluation settings. This step has been long overlooked by existing works as they often tune hyperparameters or select models directly using ID test samples \mathcal{D}_{ID}^{test} and OOD test samples \mathcal{D}_{OOD}^{test} [5, 31, 32, 6], which goes against basic machine learning principles and leads to unfair and overoptimistic results. In contrast, we use \mathcal{D}_{ID}^{val} and \mathcal{D}_{OOD}^{val} whenever applicable to ensure fairness, where \mathcal{D}_{ID}^{val} is a small subset held out from \mathcal{D}_{ID}^{test} , and \mathcal{D}_{OOD}^{val} is carefully constructed such that $\mathcal{Y}_{OOD}^{val} \cap \mathcal{Y}_{OOD}^{test} = \emptyset$.

2.2 Full-Spectrum OOD Detection

Unlike standard OOD detection which only concerns *semantic* shift between the training and test distribution, full-spectrum detection [19] further takes into account the non-semantic *covariate* shift by considering covariate-shifted ID (csID) images [20, 33, 21] (see Figure 3). Covariate-shifted samples \mathbf{x}_{csID} are non-i.i.d. w.r.t. ID samples \mathbf{x}_{ID} , yet they still semantically belong to one of the ID categories, *i.e.*, $y_{csID} \in \mathcal{Y}_{ID}$. Concrete examples of csID images include the ones that exhibit slight corruptions [20] and style changes [21].

In the full-spectrum setting, goal ① of OOD detection becomes accurate classification of both ID and csID samples from \mathcal{D}_{ID}^{test} and $\mathcal{D}_{csID}^{test}$. Meanwhile, goal ② turns into that the OOD detector should be able to flag samples from \mathcal{D}_{OOD}^{test} as OOD, while identifying samples from \mathcal{D}_{ID}^{test} and $\mathcal{D}_{csID}^{test}$.

as ID. We leverage established covariate-shifted datasets such as ImageNet-C [20] and ImageNet-R [21] to serve as $\mathcal{D}_{\text{csID}}^{\text{test}}$. The metrics for both goals remain the same as in standard OOD detection.

Remark. Essentially, the full-spectrum setting puts OOD detection into a broader scope by simultaneously considering two important distributional shifts. The standard detection setting (adopted by most prior works) ignores the covariate shift that might be encountered in the inference, and it remains unclear how current OOD detectors will respond to covariate-shifted samples. Our later results show that nearly all methods face significant performance degradation in full-spectrum detection, and we believe that this is an important problem to address.

3 Supported Benchmarks and Methods

In this section, we provide an overview of the supported benchmarks and methods in OpenOOD v1.5. Due to space limit, detailed descriptions of each benchmark and method are left in Appendix A and Appendix B, respectively.

Benchmarks. OpenOOD v1.5 supports 6 benchmarks, including 4 for standard OOD detection and 2 for full-spectrum OOD detection. The standard benchmarks are constructed with CIFAR-10, CIFAR-100, ImageNet-200, and ImageNet-1K being the ID data, respectively. The full-spectrum benchmarks are built around ImageNet-200 and ImageNet-1K, respectively. Among them, CIFAR and ImageNet-1K standard benchmark are adapted from v1 release with necessary changes for fairness and usefulness. ImageNet-200 and full-spectrum benchmarks are newly introduced in v1.5.

Comparison with prior OOD and OSR benchmarks. Most of the OOD datasets considered in previous works fall into our far-OOD category, meaning that the more difficult near-OOD detection was less emphasized than our benchmarks do. Meanwhile, we exclude problematic OOD datasets (*e.g.*, the resized version of LSUN and TIN [5] with obvious artifacts [7]) which make detection trivial and much less meaningful [7]. Following one of the seminal works [34], OSR papers often construct ID-OOD pairs by partitioning a single dataset into two splits (*e.g.*, using a 6-class subset of CIFAR-10 as ID and the other 4-class subset as OOD). While such practice is well-suited for studying near-OOD detection [35], it inevitably reduces the scale and complexity of the problem, making the resulted benchmarks less representative for real-world scenarios. In contrast, our benchmarks (especially ImageNet ones) operate at a much larger scale (in terms of the number of ID and OOD categories) than conventional OSR benchmarks.

Supported methods. By including more recent works, OpenOOD v1.5 now implements in total 40 advanced OOD detection methods within our framework. They are categorized into four groups. **Post-hoc inference methods** designs post-processors that are applied to the base classifier to generate the “OOD score” (which is then thresholded to produce the binary ID/OOD prediction). They only take effect at inference phase and by default assume that the classifier is trained with the standard cross-entropy loss. In contrast, **training methods** involve training-time regularization. Most of them assume no access to the auxiliary OOD training data (**w/o outlier data**), while some methods do (**w/ outlier data**). We also consider several **data augmentation** methods.

4 Experiment Setup

We perform extensive experiments to evaluate a wide range of methods on the supported benchmarks. This section describes the training and evaluation setup of our benchmarking experiments.

Training. For CIFAR-10/100 and ImageNet-200, we train a ResNet-18 [36] for 100 epochs. We consider the standard cross-entropy training for post-hoc methods. The optimizer is SGD with a momentum of 0.9. We use a learning rate of 0.1 with cosine annealing decay schedule [37]. A weight decay of 0.0005 is applied. The batch size is 128 for CIFAR-10/100 and 256 for ImageNet-200. Some methods have specific setup, and we adopt their official implementations and hyperparameters whenever possible.

For ImageNet-1K, we evaluate post-hoc methods with pre-trained models from torchvision [38]. In addition to ResNet-50 that is considered in OpenOOD v1, v1.5 further includes ViT [39] and Swin Transformer [40] for comprehensive evaluation. For training methods, we focus on ResNet-50 and use official checkpoints when possible. Otherwise, we fine-tune the torchvision pre-trained checkpoint for 30 epochs with a learning rate of 0.001. Again, we use a batch size of 256 and weight

decay of 0.0005. CIFAR and ImageNet models are trained using 1 and 2 Quadro RTX 6000 GPUs (24GB memory), respectively. Except ImageNet-1K experiments, we perform 3 independent training runs for each method. All training scripts are thoroughly documented in our [Github repo](#).

Evaluation. As aforementioned, we use AUROC, AUPR, and FPR@95 as metrics. In the paper we focus on near- and far-ODD AUROC which are averaged over all OOD datasets in each group. AUROC can be interpreted as the probability that the detector correctly separates ID and OOD samples; the random-guessing baseline is 50%, and the higher the better. Results under other metrics and per-dataset statistics are available in our [full result table](#). For post-hoc methods, OpenOOD supports automatic hyperparameter search using ID and OOD validation samples. The hyperparameter that yields the best AUROC is used for the final test. Evaluation scripts can be found [here](#).

Notes on missing results. The main results for standard OOD detection are presented in Table 1. A few numbers are missing for the following reasons. OpenGAN [6] has not shown success on ImageNet-1K, and substantial changes are required to make it work with ImageNet models. CSI [7], VOS [41], and NPOS [42] are infeasible with our compute resources on ImageNet. CIDER [43] and NPOS trains the CNN backbone without the final linear classifier, and the exact code for evaluating ID accuracy is not provided in their official implementations. Lastly, we do not consider training with outlier data $\mathcal{D}_{\text{OOD}}^{\text{train}}$ on ImageNet-1K since it is difficult to find OOD training samples that do not overlap with test OOD data, and no relevant methods have considered ImageNet-1K.

Table 1: Main results from OpenOOD v1.5 on standard OOD detection. In this table we use AUROC as the metric for OOD detection. Whenever applicable, we report the average number and the corresponding standard deviation obtained from 3 training runs. The best result within each group is **bolded**. Results for data augmentation methods are listed in Table 2. Full result table including other metrics and per-dataset statistics can be found [here](#).

	CIFAR-10			CIFAR-100			ImageNet-200			ImageNet-1K		
	Near-ODD	Far-ODD	ID Acc.	Near-ODD	Far-ODD	ID Acc.	Near-ODD	Far-ODD	ID Acc.	Near-ODD	Far-ODD	ID Acc.
- Post-hoc Inference Methods												
OpenMax [2] (CVPR'16)	87.62 _(±0.29)	89.62 _(±0.19)	95.06 _(±0.30)	76.41 _(±0.25)	79.48 _(±0.41)	77.25 _(±0.10)	80.27 _(±0.10)	90.20 _(±0.17)	86.37 _(±0.08)	74.77	89.26	76.18
MSP [1] (ICLR'17)	88.03 _(±0.25)	90.73 _(±0.43)	95.06 _(±0.30)	80.27 _(±0.11)	77.76 _(±0.44)	77.25 _(±0.10)	83.34 _(±0.06)	90.13 _(±0.09)	86.37 _(±0.08)	76.02	85.23	76.18
TempScale [44] (ICML'17)	88.09 _(±0.31)	90.97 _(±0.52)	95.06 _(±0.30)	80.90 _(±0.07)	78.74 _(±0.51)	77.25 _(±0.10)	83.69 _(±0.04)	90.82 _(±0.09)	86.37 _(±0.08)	77.14	87.56	76.18
ODIN [5] (ICLR'18)	82.87 _(±1.85)	87.96 _(±0.61)	95.06 _(±0.30)	79.90 _(±0.11)	79.28 _(±0.19)	77.25 _(±0.10)	80.27 _(±0.08)	91.71 _(±0.19)	86.37 _(±0.08)	74.75	89.47	76.18
MDS [31] (NeurIPS'18)	84.20 _(±2.40)	89.72 _(±1.36)	95.06 _(±0.30)	58.69 _(±0.09)	69.39 _(±1.39)	77.25 _(±0.10)	61.93 _(±0.51)	74.72 _(±0.26)	86.37 _(±0.08)	55.44	74.25	76.18
MDSEns [31] (NeurIPS'18)	60.43 _(±0.26)	73.90 _(±0.27)	95.06 _(±0.30)	46.31 _(±0.24)	66.00 _(±0.69)	77.25 _(±0.10)	54.32 _(±0.24)	69.27 _(±0.57)	86.37 _(±0.08)	49.67	67.52	76.18
RMDS [45] (arXiv'21)	89.80 _(±0.28)	92.20 _(±0.21)	95.06 _(±0.30)	80.15 _(±0.11)	82.92 _(±0.42)	77.25 _(±0.10)	82.57 _(±0.25)	88.06 _(±0.34)	86.37 _(±0.08)	76.99	86.38	76.18
Gram [46] (ICML'20)	58.66 _(±0.83)	71.73 _(±3.20)	95.06 _(±0.30)	51.66 _(±0.77)	73.36 _(±1.08)	77.25 _(±0.10)	67.67 _(±1.07)	71.19 _(±0.24)	86.37 _(±0.08)	61.70	79.71	76.18
EBO [47] (NeurIPS'20)	87.58 _(±0.46)	91.21 _(±0.92)	95.06 _(±0.30)	80.91 _(±0.08)	79.77 _(±0.61)	77.25 _(±0.10)	82.50 _(±0.05)	90.86 _(±0.21)	86.37 _(±0.08)	75.89	89.47	76.18
OpenGAN [6] (ICCV'21)	53.71 _(±1.68)	54.61 _(±15.51)	95.06 _(±0.30)	65.98 _(±1.26)	67.88 _(±1.16)	77.25 _(±0.10)	59.79 _(±3.39)	73.15 _(±4.07)	86.37 _(±0.08)	N/A	N/A	N/A
GradNorm [48] (NeurIPS'21)	54.90 _(±0.98)	57.55 _(±3.22)	95.06 _(±0.30)	70.13 _(±0.47)	69.14 _(±1.05)	77.25 _(±0.10)	72.75 _(±0.48)	84.26 _(±0.87)	86.37 _(±0.08)	72.96	90.25	76.18
ReAct [13] (NeurIPS'21)	87.11 _(±0.61)	90.42 _(±1.41)	95.06 _(±0.30)	80.77 _(±0.05)	80.39 _(±0.49)	77.25 _(±0.10)	81.87 _(±0.98)	92.31 _(±0.56)	86.37 _(±0.08)	77.38	93.67	76.18
MLS [14] (ICML'22)	87.52 _(±0.47)	91.10 _(±0.89)	95.06 _(±0.30)	81.05 _(±0.07)	79.67 _(±0.57)	77.25 _(±0.10)	82.90 _(±0.04)	91.11 _(±0.19)	86.37 _(±0.08)	76.46	89.57	76.18
KLM [14] (ICML'22)	79.19 _(±0.80)	82.68 _(±0.21)	95.06 _(±0.30)	76.56 _(±0.25)	76.24 _(±0.52)	77.25 _(±0.10)	80.76 _(±0.08)	88.53 _(±0.11)	86.37 _(±0.08)	76.64	87.60	76.18
MIL [15] (CVPR'22)	88.68 _(±0.28)	93.48 _(±0.24)	95.06 _(±0.30)	74.98 _(±0.13)	81.70 _(±0.62)	77.25 _(±0.10)	78.68 _(±0.24)	91.26 _(±0.19)	86.37 _(±0.08)	72.08	92.68	76.18
KNN [16] (ICML'22)	90.64 _(±0.20)	92.96 _(±0.14)	95.06 _(±0.30)	80.18 _(±0.15)	82.40 _(±0.17)	77.25 _(±0.10)	81.57 _(±0.17)	93.16 _(±0.22)	86.37 _(±0.08)	71.10	90.18	76.18
DICE [49] (ECCV'22)	78.34 _(±0.79)	84.23 _(±1.89)	95.06 _(±0.30)	79.38 _(±0.23)	80.01 _(±0.18)	77.25 _(±0.10)	81.78 _(±0.14)	90.80 _(±0.31)	86.37 _(±0.08)	73.07	90.95	76.18
RankFeat [50] (NeurIPS'22)	79.46 _(±2.52)	75.87 _(±5.06)	95.06 _(±0.30)	61.88 _(±1.28)	67.10 _(±1.42)	77.25 _(±0.10)	56.92 _(±1.59)	38.22 _(±3.85)	86.37 _(±0.08)	50.99	53.93	76.18
ASH [17] (ICLR'23)	75.27 _(±1.04)	78.49 _(±2.58)	95.06 _(±0.30)	78.20 _(±0.15)	80.58 _(±0.66)	77.25 _(±0.10)	82.38 _(±0.19)	93.90 _(±0.27)	86.37 _(±0.08)	78.17	95.74	76.18
SHE [18] (ICLR'23)	81.54 _(±0.51)	85.32 _(±1.43)	95.06 _(±0.30)	78.95 _(±0.18)	76.92 _(±1.16)	77.25 _(±0.10)	80.18 _(±0.25)	89.81 _(±0.61)	86.37 _(±0.08)	73.78	90.92	76.18
- Training Methods (w/o Outlier Data)												
ConfBranch [51] (arXiv'18)	89.84 _(±0.24)	92.85 _(±0.29)	94.88 _(±0.05)	71.60 _(±0.62)	68.90 _(±1.83)	76.59 _(±0.27)	79.10 _(±0.24)	90.43 _(±0.18)	85.92 _(±0.07)	70.66	83.94	75.63
RotPred [52] (NeurIPS'19)	92.68 _(±0.27)	96.62 _(±0.18)	95.35	76.43 _(±0.16)	88.40 _(±0.13)	76.03 _(±0.38)	81.59 _(±0.20)	92.56 _(±0.09)	86.37 _(±0.16)	76.52	90.00	76.55
G-ODIN [32] (CVPR'20)	89.12 _(±0.57)	95.51 _(±0.31)	94.70 _(±0.25)	77.15 _(±0.28)	85.67 _(±1.58)	74.46 _(±0.04)	77.28 _(±0.10)	92.33 _(±0.11)	84.56 _(±0.28)	70.77	85.51	74.85
CSI [7] (NeurIPS'20)	89.51 _(±0.19)	92.00 _(±0.30)	91.16 _(±0.14)	71.45 _(±0.27)	66.31 _(±1.21)	61.60 _(±0.46)	N/A	N/A	N/A	N/A	N/A	N/A
ARPL [53] (TPAMI'21)	87.44 _(±0.15)	89.31 _(±0.32)	93.66 _(±0.11)	74.94 _(±0.93)	73.69 _(±0.80)	70.70 _(±1.08)	82.02 _(±0.10)	89.23 _(±0.11)	83.95 _(±0.32)	76.30	85.50	75.87
MOS [54] (CVPR'21)	71.45 _(±3.09)	76.41 _(±5.93)	94.83 _(±0.37)	80.40 _(±0.18)	80.17 _(±1.21)	76.98 _(±0.20)	69.84 _(±0.46)	80.46 _(±0.92)	85.60 _(±0.20)	72.85	82.75	72.81
VOS [41] (ICLR'22)	87.70 _(±0.48)	90.83 _(±0.92)	94.31 _(±0.64)	80.93 _(±0.29)	81.32 _(±0.09)	77.20 _(±0.10)	82.51 _(±0.11)	91.00 _(±0.28)	86.23 _(±0.19)	N/A	N/A	N/A
LogitNorm [55] (ICML'22)	92.33 _(±0.08)	96.74 _(±0.06)	94.30 _(±0.25)	78.47 _(±0.31)	81.53 _(±1.26)	76.34 _(±0.17)	82.66 _(±0.15)	93.04 _(±0.21)	86.04 _(±0.15)	74.62	91.54	76.45
CIDER [43] (ICLR'23)	90.71 _(±0.16)	94.71 _(±0.36)	N/A	73.10 _(±0.39)	80.49 _(±0.68)	N/A	80.58 _(±1.75)	90.66 _(±1.68)	N/A	68.97	92.18	N/A
NPOS [42] (ICLR'23)	89.78 _(±0.33)	94.07 _(±0.49)	N/A	78.35 _(±0.37)	82.29 _(±1.55)	N/A	79.40 _(±0.39)	94.49 _(±0.07)	N/A	N/A	N/A	N/A
- Training Methods (w/ Outlier Data)												
OE [27] (NeurIPS'18)	94.82 _(±0.21)	96.00 _(±0.13)	94.63 _(±0.26)	88.30 _(±0.10)	81.41 _(±1.49)	76.84 _(±0.42)	84.84 _(±0.16)	89.02 _(±0.18)	85.82 _(±0.21)	N/A	N/A	N/A
MCD [28] (ICCV'19)	91.03 _(±0.12)	91.00 _(±1.10)	94.95 _(±0.04)	77.07 _(±0.32)	74.72 _(±0.78)	75.83 _(±0.04)	83.62 _(±0.09)	88.94 _(±0.10)	86.12 _(±0.17)	N/A	N/A	N/A
UDG [29] (ICCV'21)	89.91 _(±0.25)	94.06 _(±0.90)	92.36 _(±0.84)	78.02 _(±0.10)	79.59 _(±1.77)	71.54 _(±0.64)	74.30 _(±1.63)	82.09 _(±2.78)	68.11 _(±1.24)	N/A	N/A	N/A
MixOE [30] (WACV'23)	88.73 _(±0.82)	91.93 _(±0.69)	94.55 _(±0.32)	80.95 _(±0.20)	76.40 _(±1.44)	75.13 _(±0.06)	82.62 _(±0.03)	88.27 _(±0.41)	85.71 _(±0.07)	N/A	N/A	N/A

5 Analysis

In this section, we discuss multiple observations and insights that arise from the comprehensive results provided by OpenOOD v1.5. We start with standard OOD detection before delving into the full-spectrum setting.

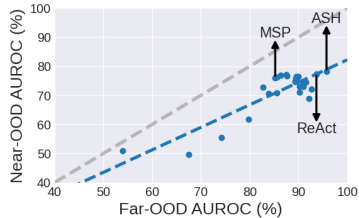


Figure 4: Near-OOD improvements are proportional to, yet slower than, far-OOD improvements on ImageNet-1K.

	ImageNet-200			ImageNet-1K			
	MSP [1]	ASH [17]	ID Acc.	MSP [1]	ReAct [13]	ASH [17]	ID Acc.
CrossEntropy	83.34 / 90.13	82.38 / 93.90	86.37	76.02 / 85.23	77.38 / 93.67	78.17 / 95.74	76.18
StyleAugment [22]	80.99 / 88.44	80.65 / 93.70	83.41	75.78 / 85.73	76.70 / 91.88	78.21 / 94.90	74.68
RandAugment [23]	83.17 / 90.34	81.56 / 94.53	86.58	76.60 / 85.27	78.30 / 93.50	79.81 / 95.01	76.90
AugMix [24]	83.49 / 90.68	82.87 / 94.66	87.01	77.49 / 86.67	79.94 / 93.70	82.16 / 96.05	77.63
DeepAugment [21]	81.39 / 88.79	80.61 / 93.84	85.00	76.67 / 86.26	78.43 / 92.12	79.14 / 93.90	76.77
PixMix [25]	82.15 / 90.23	81.36 / 95.01	85.79	76.86 / 85.63	79.12 / 91.59	78.92 / 92.17	77.44
RegMixup [26]	84.13 / 90.81	79.38 / 92.74	87.25	77.04 / 86.31	77.68 / 92.45	78.45 / 95.35	76.68

Table 2: Data augmentation methods (column headers) are beneficial for OOD detection and amplify the performance gain when combined with post-hoc methods (row headers). The cell numbers represent the near-OOD / far-OOD AUROC.

5.1 Standard Detection

No single winner. In Table 1, there is no single method that consistently outperforms others across benchmarks, and the ranking can be quite different from one dataset to another. For example, ReAct [13] and ASH [17] are extremely powerful on ImageNet but less competitive on CIFAR. In contrast, methods that yield remarkable performance on small datasets (*e.g.*, KNN [16] and RotPred [52]) do not show clear advantage on large datasets. This observation further emphasizes the importance of evaluation in large-scale settings as they better approximate complex scenarios in the real world.

Data augmentations help. While data augmentations have been shown beneficial for standard classification [23] and OOD generalization [22, 24, 21, 25, 26], their effects for OOD detection remain unclear. In Table 2, we find that several data augmentation methods, despite not being designed to improve OOD detection, can actually boost detection rates in many cases. More interestingly, the performance gain is amplified when they are combined with powerful post-processors. For example, compared with the baseline of cross-entropy training on ImageNet-1K near-OOD, AugMix [24] achieves $76.02 + 1.47 = 77.49\%$ AUROC and $78.17 + 3.99 = 82.16\%$ AUROC when working with MSP [1] and ASH [17], respectively. 82.16% is the current best score among all methods. The results indicate that the effects from data augmentations and post-processors are complementary.

Near-OOD remains more challenging than far-OOD. Figure 4 plots the trend of near-OOD AUROC v.s far-OOD AUROC on ImageNet-1K. Not surprisingly, near-OOD AUROC is (roughly) proportional to far-OOD AUROC, meaning that the improvement for one group is likely to help with the other as well. Meanwhile, we notice that the progress on near-OOD is slower than that on far-OOD. Besides the fact that near-OOD detection is more difficult, this may also be due to that previous works mainly focus on far-OOD datasets when designing and evaluating their methods.

Vision transformers do not outperform ResNets. We visualize in Figure 5 the performance of a few powerful post-hoc methods on ImageNet-1K with ResNet-50, ViT-B-16 [39], and Swin-T [40] as the classifier. We use the ImageNet-1K-pre-trained checkpoints provided by torchvision. As reference, they have 25.6M, 86.6M, and 28.3M parameters, and their ID accuracy is 76.18%, 81.14%, and 81.59%, respectively. Interestingly, despite their better ID classification performance, we find that vision transformers do *not* show noticeable improvements over ResNets for OOD detection, which aligns with the observation in [14]. Meanwhile, different post-processor may favor different architecture. For instance, the top-2 post-processor on ResNet-50, *i.e.*, ASH [17] and ReAct [13], both have significant performance when operating on transformer. RMDS [45], in contrast, suits transformers much better than ResNets.

Training methods excel at small datasets. On CIFAR-10/100, we find that training-time regularizations (the second group in Table 1) can provide better OOD detection capability than post-hoc methods. In particular, RotPred [52] and LogitNorm [55] stand out as two powerful training methods (without using outlier data). On CIFAR-10, they both lead to $\sim 2\%$ and $\sim 3\%$ increase in near- and far-OOD AUROC, respectively, compared to the best-performing post-processors. Meanwhile, however, training methods in general do not outperform post-hoc ones on ImageNet-200/1K. This might be due to that more sophisticated training dynamics require larger models or longer training, and the exact reason needs further investigation in future works.

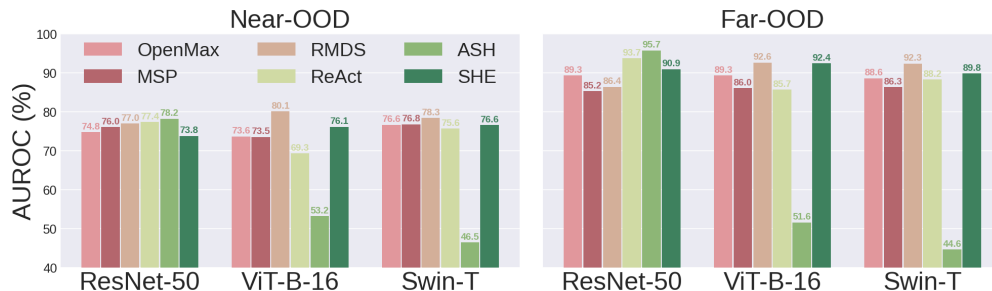


Figure 5: OOD detection rates of post-hoc methods with different architectures on ImageNet-1K. Some methods are sensitive to model architecture while some are not. Transformers do not seem to have clear advantage over ResNets.

Post-hoc methods are more effective for large-scale settings. This is particularly true on ImageNet-1K, where applying post-processors to a model pre-trained with the standard cross-entropy loss are the top-performing solutions for both near- and far-OOD detection, according to Table 1.

Outlier data helps in certain cases. Compared with methods that do not have such consideration, incorporating OOD training data (the last group in Table 1) is helpful mainly when the test OOD samples are similar to the training ones. For instance, OE [27] yields the highest near-OOD AUROC on CIFAR-100 because the used OOD training set (TIN-597; see Appendix A for details) is similar to one of the near-OOD test sets (TIN). In contrast, it does not seem to be beneficial for detecting far-OOD samples (which are quite different from TIN images) and actually underperforms several other methods which do not use the outlier data.

ID accuracy can be affected a little. Lastly, as shown in Table 1, most training methods incur slight drop (within 1%) in ID classification accuracy compared to the standard cross-entropy training. For some methods the drop could be large, and it is important for future works to monitor ID accuracy to maintain utility while improving OOD detection capability.

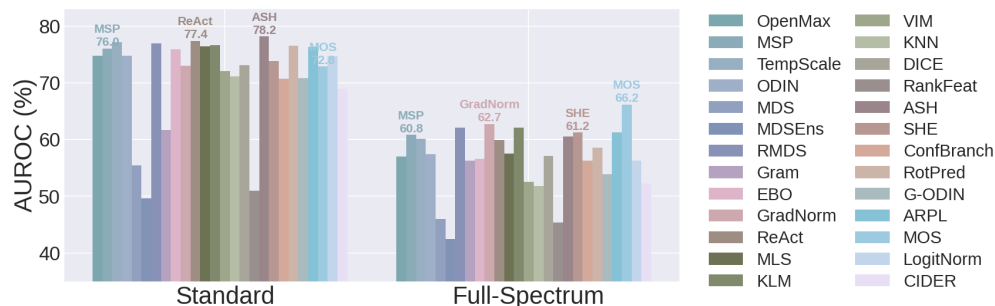


Figure 6: Comparison between standard and full-spectrum detection on ImageNet-1K (near-OOD). Many detectors suffer significant performance degradation in the full-spectrum setting.

5.2 Full-Spectrum Detection

Full-spectrum detection poses challenge for current detectors. This can be seen in Figure 6, where the near-OOD AUROC of most methods decreases by >10% on ImageNet-1K (similar trend holds for far-OOD; see full results here). The performance drop suggests that *existing OOD detectors can be sensitive to the non-semantic covariate shift and are likely to flag covariate-shifted ID samples as OOD*. Such behaviour is not ideal because: 1) It does not align with human perception/decision (e.g., a human annotator classifying dog and car wouldn't mark a covariate-shifted dog image as something unknown or novel). 2) It can harm the classifier's generalization capability on covariate-shifted ID data, as often times it is assumed that the classifier would refrain from making predictions when the sample is identified as OOD (or at least the OOD flag associated with the prediction would indicate its unreliability). As a result, we firmly believe that full-spectrum detection is an important open problem for ensuring human-model alignment and the model's practical reliability. One method

that stands out in this resort is MOS [54], which utilizes a two-level semantic hierarchy to facilitate classification and OOD detection. MOS exhibits the smallest performance drop when changing from standard to full-spectrum detection (from 72.85% to 66.17% in AUROC) and serves as a strong baseline for future works to tackle full-spectrum detection.

Data augmentations continue to help in full-spectrum settings.

Similar to our observations in standard OOD detection, in Table 3 we see that data augmentations also boost full-spectrum detection rates especially when combined with powerful post-hoc methods. For example, compared to the cross-entropy baseline, while AugMix [24] increases near-OOD AUROC “only” by 2.35% with the MSP detector [1], it leads to a much significant improvement of 8.45% when working with SHE [18]. AugMix + SHE is the current best approach in terms of full-spectrum near-OOD AUROC on ImageNet-1K. In the meantime, we do notice that data augmentations do not clearly benefits full-spectrum far-OOD AUROC, and the reasons require future study. That said, our results demonstrate that in general “data augmentation + post-processor” is promising for both standard and full-spectrum OOD detection.

Table 3: ImageNet-1K full-spectrum detection results of data augmentation methods. The numbers in each cell represent the near-OOD / far-OOD AUROC. Again, they are helpful especially when combined with appropriate post-processors and when performing near-OOD detection.

	MSP [1]	GradNorm [56]	SHE [18]	ID Acc.
CrossEntropy	60.79 / 72.32	62.70 / 83.49	61.21 / 83.04	54.35
StyleAugment [22]	62.09 / 74.37	65.27 / 81.62	66.64 / 82.64	55.44
RandAugment [23]	61.36 / 72.07	63.27 / 76.08	64.41 / 76.68	55.57
AugMix [24]	63.14 / 74.62	67.10 / 81.29	69.66 / 83.06	57.46
DeepAugment [21]	63.51 / 75.40	65.66 / 76.27	68.27 / 78.85	57.82
PixMix [25]	62.51 / 73.47	61.07 / 70.00	65.02 / 77.03	57.27
RegMixup [26]	61.32 / 72.87	61.86 / 79.98	64.71 / 81.23	55.55

6 Conclusion and Discussion

In this work we present OpenOOD v1.5, which enhances its earlier version by 1) providing results on the large-scale ImageNet, 2) investigating full-spectrum detection, and 3) introducing new features such as the leaderboard. We highlight several insights regarding the current state and future directions for OOD detection: **1)** A single winner that leads to superior performance across multiple benchmarks is still missing. **2)** Data augmentations are quite effective for improving OOD detection capability, and the combination of data augmentation with strong post-processor seems promising. **3)** Near-OOD remains more challenging than far-OOD, yet their improvement is proportional to each other. **4)** Full-spectrum detection poses challenge for existing methods. We hope that the codebase, benchmark, evaluation results, and insights of OpenOOD can accelerate the progress and foster collective efforts towards advancing the state-of-the-art in OOD detection.

Related work. To the best of our knowledge, OpenOOD v1.5 is the only work that comprehensively evaluates a wide range of OOD detection methods on multiple benchmarks of various sizes. We discuss a few works that relate to OpenOOD in certain aspects in Appendix C.

Limitation. In this work we focus on the context where there assumes to be a discriminative classifier for the ID classification in the first place. As a result, all the OOD detection methods considered in our work are discriminative. OOD detection approaches that are based on generative modeling (e.g., [57, 58, 59, 60]) are not currently included in OpenOOD.

Societal Impact. OOD detection is an important topic for machine learning safety as it studies how deep neural networks can handle unknown inputs desirably. As an open-sourced, unified, and comprehensive benchmark for OOD detection, OpenOOD is expected to benefit the whole community and facilitate relevant research, which we believe has positive societal impacts.

Future Work. First, we will keep maintaining OpenOOD’s codebase and leaderboard. The codebase is hosted on Github, and the leaderboard is hosted using Github pages, which both are free services. We anticipate the benchmark to be community-driven: Reporting new results and submitting new entries to the leaderboard would be easy with our unified evaluator.

In addition to the maintenance, in the future v2 release we plan to extend the scope of OpenOOD beyond image classification and include more application scenarios such as object detection, semantic segmentation, and natural language processing tasks. Specifically, it would be interesting to see whether current OOD detectors, which are designed for image classifiers, can generalize to different problems and modalities.

Acknowledgments and Disclosure of Funding

This study is supported by the Ministry of Education, Singapore, under its MOE AcRF Tier 2 (MOE-T2EP20221- 0012), NTU NAP, and under the RIE2020 Industry Alignment Fund – Industry Collaboration Projects (IAF-ICP) Funding Initiative, as well as cash and in-kind contribution from the industry partner(s).

References

- [1] Dan Hendrycks and Kevin Gimpel. A baseline for detecting misclassified and out-of-distribution examples in neural networks. In *ICLR*, 2017. 1, 6, 7, 9, 16, 17
- [2] Abhijit Bendale and Terrance E Boult. Towards open set deep networks. In *CVPR*, 2016. 1, 6, 16, 17
- [3] Jingkang Yang, Kaiyang Zhou, Yixuan Li, and Ziwei Liu. Generalized out-of-distribution detection: A survey. *arXiv preprint arXiv:2110.11334*, 2021. 1
- [4] Pramuditha Perera and Vishal M Patel. Deep transfer learning for multiple class novelty detection. In *Proceedings of the IEEE/CVF Conference on Computer Vision and Pattern Recognition*, pages 11544–11552, 2019. 2
- [5] Shiyu Liang, Yixuan Li, and Rayadurgam Srikant. Enhancing the reliability of out-of-distribution image detection in neural networks. In *ICLR*, 2018. 2, 4, 5, 6, 16, 17, 18
- [6] Shu Kong and Deva Ramanan. Opengan: Open-set recognition via open data generation. In *ICCV*, 2021. 2, 4, 6, 17
- [7] Jihoon Tack, Sangwoo Mo, Jongheon Jeong, and Jinwoo Shin. Csi: Novelty detection via contrastive learning on distributionally shifted instances. In *NeurIPS*, 2020. 2, 5, 6, 17, 18
- [8] Jingkang Yang, Pengyun Wang, Dejian Zou, Zitang Zhou, Kunyuan Ding, WenXuan Peng, Haoqi Wang, Guangyao Chen, Bo Li, Yiyu Sun, Xuefeng Du, Kaiyang Zhou, Wayne Zhang, Dan Hendrycks, Yixuan Li, and Ziwei Liu. OpenOOD: Benchmarking generalized out-of-distribution detection. In *Thirty-sixth Conference on Neural Information Processing Systems Datasets and Benchmarks Track*, 2022. URL https://openreview.net/forum?id=gT6j4_tskUt. 2, 15
- [9] Li Deng. The mnist database of handwritten digit images for machine learning research. *IEEE Signal Processing Magazine*, 2012. 2, 15
- [10] Alex Krizhevsky, Geoffrey Hinton, et al. Learning multiple layers of features from tiny images. 2009. 2, 15
- [11] Alex Krizhevsky, Vinod Nair, and Geoffrey Hinton. Cifar-10 and cifar-100 datasets. URL: <https://www.cs.toronto.edu/kriz/cifar.html>, 6(1):1, 2009. 2, 15
- [12] Jia Deng, Wei Dong, Richard Socher, Li-Jia Li, Kai Li, and Li Fei-Fei. Imagenet: A large-scale hierarchical image database. In *2009 IEEE conference on computer vision and pattern recognition*, pages 248–255. Ieee, 2009. 2, 15
- [13] Yiyu Sun, Chuan Guo, and Yixuan Li. React: Out-of-distribution detection with rectified activations. In *NeurIPS*, 2021. 2, 6, 7, 16, 17
- [14] Dan Hendrycks, Steven Basart, Mantas Mazeika, Mohammadreza Mostajabi, Jacob Steinhardt, and Dawn Song. Scaling out-of-distribution detection for real-world settings. In *ICML*, 2022. 2, 6, 7, 15, 16, 17
- [15] Haoqi Wang, Zhizhong Li, Litong Feng, and Wayne Zhang. Vim: Out-of-distribution with virtual-logit matching. In *CVPR*, 2022. 2, 6, 15, 16, 17
- [16] Yiyu Sun, Yifei Ming, Xiaojin Zhu, and Yixuan Li. Out-of-distribution detection with deep nearest neighbors. *ICML*, 2022. 2, 6, 7, 16, 17
- [17] Andrija Djuricic, Nebojsa Bozanic, Arjun Ashok, and Rosanne Liu. Extremely simple activation shaping for out-of-distribution detection. In *The Eleventh International Conference on Learning Representations*, 2023. URL <https://openreview.net/forum?id=ndYXTEL6cZz>. 2, 6, 7, 16, 17
- [18] Jinsong Zhang, Qiang Fu, Xu Chen, Lun Du, Zelin Li, Gang Wang, xiaoguang Liu, Shi Han, and Dongmei Zhang. Out-of-distribution detection based on in-distribution data patterns memorization with modern hopfield energy. In *The Eleventh International Conference on Learning Representations*, 2023. URL <https://openreview.net/forum?id=KkazG4lgKL>. 2, 6, 9, 16, 17

- [19] Jingkang Yang, Kaiyang Zhou, and Ziwei Liu. Full-spectrum out-of-distribution detection. *arXiv preprint arXiv:2204.05306*, 2022. 3, 4
- [20] Dan Hendrycks and Thomas Dietterich. Benchmarking neural network robustness to common corruptions and perturbations. *Proceedings of the International Conference on Learning Representations*, 2019. 3, 4, 5, 15
- [21] Dan Hendrycks, Steven Basart, Norman Mu, Saurav Kadavath, Frank Wang, Evan Dorundo, Rahul Desai, Tyler Zhu, Samyak Parajuli, Mike Guo, Dawn Song, Jacob Steinhardt, and Justin Gilmer. The many faces of robustness: A critical analysis of out-of-distribution generalization. *ICCV*, 2021. 3, 4, 5, 7, 9, 15, 16, 17
- [22] Robert Geirhos, Patricia Rubisch, Claudio Michaelis, Matthias Bethge, Felix A. Wichmann, and Wieland Brendel. Imagenet-trained CNNs are biased towards texture; increasing shape bias improves accuracy and robustness. In *International Conference on Learning Representations*, 2019. URL <https://openreview.net/forum?id=Bygh9j09KX>. 3, 7, 9, 17
- [23] Ekin D Cubuk, Barret Zoph, Jonathon Shlens, and Quoc V Le. Randaugment: Practical automated data augmentation with a reduced search space. In *Proceedings of the IEEE/CVF conference on computer vision and pattern recognition workshops*, pages 702–703, 2020. 3, 7, 9, 17
- [24] Dan Hendrycks, Norman Mu, Ekin D. Cubuk, Barret Zoph, Justin Gilmer, and Balaji Lakshminarayanan. AugMix: A simple data processing method to improve robustness and uncertainty. *Proceedings of the International Conference on Learning Representations (ICLR)*, 2020. 3, 7, 9, 17
- [25] Dan Hendrycks, Andy Zou, Mantas Mazeika, Leonard Tang, Dawn Song, and Jacob Steinhardt. Pixmix: Dreamlike pictures comprehensively improve safety measures. *arXiv preprint arXiv:2112.05135*, 2021. 3, 7, 9, 17
- [26] Francesco Pinto, Harry Yang, Ser-Nam Lim, Philip Torr, and Puneet K. Dokania. Using mixup as a regularizer can surprisingly improve accuracy & out-of-distribution robustness. In Alice H. Oh, Alekh Agarwal, Danielle Belgrave, and Kyunghyun Cho, editors, *Advances in Neural Information Processing Systems*, 2022. URL <https://openreview.net/forum?id=5j6fWcPcc0>. 3, 7, 9, 18
- [27] Dan Hendrycks, Mantas Mazeika, and Thomas Dietterich. Deep anomaly detection with outlier exposure. In *ICLR*, 2019. 4, 6, 8, 16, 17
- [28] Qing Yu and Kiyoharu Aizawa. Unsupervised out-of-distribution detection by maximum classifier discrepancy. In *ICCV*, 2019. 4, 6, 16, 17
- [29] Jingkang Yang, Haoqi Wang, Litong Feng, Xiaopeng Yan, Huabin Zheng, Wayne Zhang, and Ziwei Liu. Semantically coherent out-of-distribution detection. In *ICCV*, 2021. 4, 6, 15, 16, 17
- [30] Jingyang Zhang, Nathan Inkawhich, Randolph Linderman, Yiran Chen, and Hai Li. Mixture outlier exposure: Towards out-of-distribution detection in fine-grained environments. In *Proceedings of the IEEE/CVF Winter Conference on Applications of Computer Vision (WACV)*, pages 5531–5540, January 2023. 4, 6, 16, 17
- [31] Kimin Lee, Kibok Lee, Honglak Lee, and Jinwoo Shin. A simple unified framework for detecting out-of-distribution samples and adversarial attacks. In *NeurIPS*, 2018. 4, 6, 16, 17
- [32] Yen-Chang Hsu, Yilin Shen, Hongxia Jin, and Zolt Kira. Generalized odin: Detecting out-of-distribution image without learning from out-of-distribution data. In *CVPR*, 2020. 4, 6, 17
- [33] Benjamin Recht, Rebecca Roelofs, Ludwig Schmidt, and Vaishal Shankar. Do imagenet classifiers generalize to imagenet? In *International conference on machine learning*, pages 5389–5400. PMLR, 2019. 4, 15
- [34] Lawrence Neal, Matthew Olson, Xiaoli Fern, Weng-Keen Wong, and Fuxin Li. Open set learning with counterfactual images. In *ECCV*, 2018. 5
- [35] Faruk Ahmed and Aaron Courville. Detecting semantic anomalies. In *AAAI*, 2020. 5
- [36] Kaiming He, Xiangyu Zhang, Shaoqing Ren, and Jian Sun. Deep residual learning for image recognition. In *CVPR*, 2016. 5
- [37] Ilya Loshchilov and Frank Hutter. Sgdr: Stochastic gradient descent with warm restarts. *arXiv preprint arXiv:1608.03983*, 2016. 5

- [38] TorchVision maintainers and contributors. Torchvision: Pytorch’s computer vision library. <https://github.com/pytorch/vision>, 2016. 5
- [39] Alexey Dosovitskiy, Lucas Beyer, Alexander Kolesnikov, Dirk Weissenborn, Xiaohua Zhai, Thomas Unterthiner, Mostafa Dehghani, Matthias Minderer, Georg Heigold, Sylvain Gelly, Jakob Uszkoreit, and Neil Houlsby. An image is worth 16x16 words: Transformers for image recognition at scale. In *International Conference on Learning Representations*, 2021. URL <https://openreview.net/forum?id=YicbFdNTTy>. 5, 7
- [40] Ze Liu, Yutong Lin, Yue Cao, Han Hu, Yixuan Wei, Zheng Zhang, Stephen Lin, and Baining Guo. Swin transformer: Hierarchical vision transformer using shifted windows. In *Proceedings of the IEEE/CVF international conference on computer vision*, pages 10012–10022, 2021. 5, 7
- [41] Xuefeng Du, Zhaoning Wang, Mu Cai, and Yixuan Li. Vos: Learning what you don’t know by virtual outlier synthesis. In *ICLR*, 2022. 6, 17
- [42] Leitian Tao, Xuefeng Du, Jerry Zhu, and Yixuan Li. Non-parametric outlier synthesis. In *The Eleventh International Conference on Learning Representations*, 2023. URL <https://openreview.net/forum?id=JHk1pEZqduQ>. 6, 17
- [43] Yifei Ming, Yiyun Sun, Ousmane Dia, and Yixuan Li. How to exploit hyperspherical embeddings for out-of-distribution detection? In *The Eleventh International Conference on Learning Representations*, 2023. URL <https://openreview.net/forum?id=aEFaE0W5pAd>. 6, 17
- [44] Chuan Guo, Geoff Pleiss, Yu Sun, and Kilian Q Weinberger. On calibration of modern neural networks. In *ICML*, 2017. 6, 16, 17
- [45] Jie Ren, Stanislav Fort, Jeremiah Liu, Abhijit Guha Roy, Shreyas Padhy, and Balaji Lakshminarayanan. A simple fix to mahalanobis distance for improving near-ood detection. *arXiv preprint arXiv:2106.09022*, 2021. 6, 7, 16, 17
- [46] Chandramouli Shama Sastry and Sageev Oore. Detecting out-of-distribution examples with gram matrices. In *ICML*, 2020. 6, 16, 17
- [47] Weitang Liu, Xiaoyun Wang, John D Owens, and Yixuan Li. Energy-based out-of-distribution detection. In *NeurIPS*, 2020. 6, 16, 17
- [48] Rui Huang, Andrew Geng, and Yixuan Li. On the importance of gradients for detecting distributional shifts in the wild. In *NeurIPS*, 2021. 6, 16
- [49] Yiyun Sun and Sharon Li. Dice: Leveraging sparsification for out-of-distribution detection. In *ECCV*, 2022. 6, 16, 17
- [50] Yue Song, Nicu Sebe, and Wei Wang. Rankfeat: Rank-1 feature removal for out-of-distribution detection. In Alice H. Oh, Alekh Agarwal, Danielle Belgrave, and Kyunghyun Cho, editors, *Advances in Neural Information Processing Systems*, 2022. URL <https://openreview.net/forum?id=-deKNiSOXLG>. 6, 16, 17
- [51] Terrance DeVries and Graham W Taylor. Learning confidence for out-of-distribution detection in neural networks. *arXiv preprint arXiv:1802.04865*, 2018. 6, 17
- [52] Dan Hendrycks, Mantas Mazeika, Saurav Kadavath, and Dawn Song. Using self-supervised learning can improve model robustness and uncertainty. In H. Wallach, H. Larochelle, A. Beygelzimer, F. d’Alché-Buc, E. Fox, and R. Garnett, editors, *Advances in Neural Information Processing Systems*, volume 32. Curran Associates, Inc., 2019. URL https://proceedings.neurips.cc/paper_files/paper/2019/file/a2b15837edac15df90721968986f7f8e-Paper.pdf. 6, 7, 17
- [53] Guangyao Chen, Peixi Peng, Xiangqian Wang, and Yonghong Tian. Adversarial reciprocal points learning for open set recognition. *arXiv preprint arXiv:2103.00953*, 2021. 6, 17
- [54] Rui Huang and Yixuan Li. Mos: Towards scaling out-of-distribution detection for large semantic space. In *CVPR*, 2021. 6, 9, 15, 17
- [55] Hongxin Wei, Renchunzi Xie, Hao Cheng, Lei Feng, Bo An, and Yixuan Li. Mitigating neural network overconfidence with logit normalization. In *ICML*, 2022. 6, 7, 17
- [56] Rui Huang, Andrew Geng, and Yixuan Li. On the importance of gradients for detecting distributional shifts in the wild. In *NeurIPS*, 2021. 9, 17

- [57] Ev Zisselman and Aviv Tamar. Deep residual flow for out of distribution detection. In *CVPR*, 2020. 9
- [58] Polina Kirichenko, Pavel Izmailov, and Andrew Gordon Wilson. Why normalizing flows fail to detect out-of-distribution data. In *NeurIPS*, 2020. 9
- [59] Eric Nalisnick, Akihiro Matsukawa, Yee Whye Teh, Dilan Gorur, and Balaji Lakshminarayanan. Do deep generative models know what they don’t know? In *NeurIPS*, 2018. 9
- [60] Joan Serrà, David Álvarez, Vicenç Gómez, Olga Slizovskaia, José F Núñez, and Jordi Luque. Input complexity and out-of-distribution detection with likelihood-based generative models. 2020. 9
- [61] Ya Le and Xuan Yang. Tiny imagenet visual recognition challenge. *CS 231N*, 7(7):3, 2015. 15
- [62] Yuval Netzer, Tao Wang, Adam Coates, Alessandro Bissacco, Bo Wu, and Andrew Y Ng. Reading digits in natural images with unsupervised feature learning. 2011. 15
- [63] M. Cimpoi, S. Maji, I. Kokkinos, S. Mohamed, , and A. Vedaldi. Describing textures in the wild. In *Proceedings of the IEEE Conf. on Computer Vision and Pattern Recognition (CVPR)*, 2014. 15
- [64] Bolei Zhou, Agata Lapedriza, Aditya Khosla, Aude Oliva, and Antonio Torralba. Places: A 10 million image database for scene recognition. *IEEE Transactions on Pattern Analysis and Machine Intelligence*, 2017. 15
- [65] Sagar Vaze, Kai Han, Andrea Vedaldi, and Andrew Zisserman. Open-set recognition: A good closed-set classifier is all you need. In *ICLR*, 2022. 15
- [66] Grant Van Horn, Oisín Mac Aodha, Yang Song, Yin Cui, Chen Sun, Alex Shepard, Hartwig Adam, Pietro Perona, and Serge Belongie. The inaturalist species classification and detection dataset. In *Proceedings of the IEEE conference on computer vision and pattern recognition*, pages 8769–8778, 2018. 15
- [67] Jianxiong Xiao, James Hays, Krista A Ehinger, Aude Oliva, and Antonio Torralba. Sun database: Large-scale scene recognition from abbey to zoo. In *2010 IEEE computer society conference on computer vision and pattern recognition*, pages 3485–3492. IEEE, 2010. 15
- [68] Julian Bitterwolf, Maximilian Müller, and Matthias Hein. In or out? fixing imagenet out-of-distribution detection evaluation. *arXiv preprint arXiv:2306.00826*, 2023. 15, 16, 18
- [69] Tal Ridnik, Emanuel Ben-Baruch, Asaf Noy, and Lihí Zelnik-Manor. Imagenet-21k pretraining for the masses, 2021. 15
- [70] Alina Kuznetsova, Hassan Rom, Neil Alldrin, Jasper Uijlings, Ivan Krasin, Jordi Pont-Tuset, Shahab Kamali, Stefan Popov, Matteo Mallocci, Alexander Kolesnikov, et al. The open images dataset v4: Unified image classification, object detection, and visual relationship detection at scale. *International Journal of Computer Vision*, 128(7):1956–1981, 2020. 15
- [71] George A Miller. Wordnet: a lexical database for english. *Communications of the ACM*, 38(11):39–41, 1995. 16
- [72] Fahim Tajwar, Ananya Kumar, Sang Michael Xie, and Percy Liang. No true state-of-the-art? ood detection methods are inconsistent across datasets. *arXiv preprint arXiv:2109.05554*, 2021. 18
- [73] Ido Galil, Mohammed Dabbah, and Ran El-Yaniv. A framework for benchmarking class-out-of-distribution detection and its application to imagenet. In *The Eleventh International Conference on Learning Representations*, 2023. URL <https://openreview.net/forum?id=Iuubb9W6Jtk>. 18
- [74] Konstantin Kirchheim, Marco Filax, and Frank Ortmeier. Pytorch-ood: A library for out-of-distribution detection based on pytorch. In *Proceedings of the IEEE/CVF Conference on Computer Vision and Pattern Recognition (CVPR) Workshops*, pages 4351–4360, June 2022. 18

Checklist

1. For all authors...
 - (a) Do the main claims made in the abstract and introduction accurately reflect the paper’s contributions and scope? [Yes]
 - (b) Did you describe the limitations of your work? [Yes] See Section 6.
 - (c) Did you discuss any potential negative societal impacts of your work? [Yes] See Section 6.
 - (d) Have you read the ethics review guidelines and ensured that your paper conforms to them? [Yes]
2. If you are including theoretical results...
 - (a) Did you state the full set of assumptions of all theoretical results? [N/A]
 - (b) Did you include complete proofs of all theoretical results? [N/A]
3. If you ran experiments (e.g. for benchmarks)...
 - (a) Did you include the code, data, and instructions needed to reproduce the main experimental results (either in the supplemental material or as a URL)? [Yes] See our [code repo](#).
 - (b) Did you specify all the training details (e.g., data splits, hyperparameters, how they were chosen)? [Yes] See our [code repo](#).
 - (c) Did you report error bars (e.g., with respect to the random seed after running experiments multiple times)? [Yes] See Table 1.
 - (d) Did you include the total amount of compute and the type of resources used (e.g., type of GPUs, internal cluster, or cloud provider)? [Yes] See Section 4.
4. If you are using existing assets (e.g., code, data, models) or curating/releasing new assets...
 - (a) If your work uses existing assets, did you cite the creators? [Yes]
 - (b) Did you mention the license of the assets? [N/A]
 - (c) Did you include any new assets either in the supplemental material or as a URL? [N/A]
 - (d) Did you discuss whether and how consent was obtained from people whose data you’re using/curating? [N/A]
 - (e) Did you discuss whether the data you are using/curating contains personally identifiable information or offensive content? [N/A]
5. If you used crowdsourcing or conducted research with human subjects...
 - (a) Did you include the full text of instructions given to participants and screenshots, if applicable? [N/A]
 - (b) Did you describe any potential participant risks, with links to Institutional Review Board (IRB) approvals, if applicable? [N/A]
 - (c) Did you include the estimated hourly wage paid to participants and the total amount spent on participant compensation? [N/A]

A Benchmark Breakdown

We describe each benchmark in detail in this section.

CIFAR-10. The first benchmark considers CIFAR-10 [10] as ID. We use the official train set as $\mathcal{D}_{\text{ID}}^{\text{train}}$ and hold out 1,000 samples from the test set to form $\mathcal{D}_{\text{ID}}^{\text{val}}$, while the remaining 9,000 test samples are taken as $\mathcal{D}_{\text{ID}}^{\text{test}}$. The *near*-OOD group contains CIFAR-100 [11] and Tiny ImageNet (TIN) [61]. 1,203 images are removed from TIN due to the overlap with CIFAR [29]. Another 1,000 TIN images covering 20 categories are held out to serve as $\mathcal{D}_{\text{OOD}}^{\text{val}}$ which is disjoint with $\mathcal{D}_{\text{OOD}}^{\text{test}}$. The *far*-OOD group consists of MNIST [9], SVHN [62], Textures [63], and Places365 [64] with 1,305 images removed due to semantic overlap [8]. The OOD group is determined by image content and semantics: Near-OOD images are similar to CIFAR-10 as they all include specific objects, while far-OOD images are either numerical digits, textural patterns, or scene imagery.

CIFAR-100. The CIFAR-100 benchmark is similar to the CIFAR-10 one. We take 1,000 samples out of the ID test set as ID validation data. The *near*-OOD split is made of CIFAR-10 and TIN. The *far*-OOD group is the same as for CIFAR-10.

ImageNet-1K. We use 45K images from the ImageNet validation set [12] as $\mathcal{D}_{\text{ID}}^{\text{test}}$, while the remaining 5K images serve as $\mathcal{D}_{\text{ID}}^{\text{val}}$. We do not modify the original 1.2M ImageNet training set such that any pre-trained models can be evaluated fairly with OpenOOD. Several datasets have been commonly used as OOD datasets for ImageNet-1K, including Species [14], Semantic Shift Benchmark (SSB) [65], Textures [63], OpenImage-O [15], and iNaturalist [66], Places [64], and SUN [67] (the curated versions from [54]).

However, a recent work [68] points out that some of these datasets are noisy, *i.e.*, they contain samples that either belong to a certain ID category or exhibit ID objects. Their observation is made by manually inspecting 400 random images from each dataset, and the extent to which such “noise” affects the results obtained on the global, full dataset remains unclear. To see this, in Table 4 we compare the OOD detection results computed on either 1) the original, full OOD dataset or 2) the tiny subset (selected from the 400 random samples; only has a few hundreds of samples) that is verified by [68] to be indeed OOD. On one hand, it can be seen that the detection AUROC on the “clean” version of Species and Places are a lot higher (with >10% and >5% difference) than that on their respect full version, indicating that indeed these two datasets include many ID samples and can severely underestimate the OOD detection performance. On the other hand, datasets like SSB-hard (the hard split of SSB), iNaturalist, Textures, and OpenImage-O do not show noticeably different result between their full and clean version, which suggests that the small number of noisy samples from the 400 random images have much less effect when considering the large full dataset. As a result, we posit that it is still reasonable to use the full SSB-hard, iNaturalist, Textures, and OpenImage-O as OOD datasets for ImageNet-1K.

We include SSB-hard [65] and NINCO [68] in the *near*-OOD group for ImageNet-1K. SSB-hard consists of 49K images and covers 980 categories selected from ImageNet-21K [69]. NINCO is a new dataset of 5879 images curated by Bitterwolf et al. [68] and is manually inspected to be noise-free. The *far*-OOD group considers iNaturalist [66], Textures [63], and OpenImage-O [15]. The first two datasets were first used as benchmarks in the MOS paper [54] and later have become popular for evaluating ImageNet models. OpenImage-O is curated from Open Images [70]. 1,763 images from OpenImage-O are picked out as $\mathcal{D}_{\text{OOD}}^{\text{val}}$. Unlike CIFAR, for ImageNet which has 1K diverse visual categories, it is hard to define near/far-OOD based on label semantics. Instead, here we make the categorization according to the empirical difficulty that we observe in experiments.

ImageNet-1K (full-spectrum). The only difference with the standard benchmark is that we further include covariate-shifted ID samples $\mathcal{D}_{\text{csID}}^{\text{test}}$ and consider $\mathcal{D}_{\text{csID}}^{\text{test}}$ and $\mathcal{D}_{\text{ID}}^{\text{test}}$ together as ID. We use three different $\mathcal{D}_{\text{csID}}^{\text{test}}$: ImageNet-C [20] with image corruptions, ImageNet-R [21] with style changes, and ImageNet-V2 [33] with resampling bias. They are all commonly used for evaluating classifiers’ ability to generalize to covariate-shifted ID images. ImageNet-C has 15 corruption types each with 5 severities. We randomly sample 10K images uniformly across the 75 combinations to form the test set that is used in OpenOOD. OOD datasets remain the same so that a straight comparison can be made between the standard and full-spectrum setting.

ImageNet-200 and the full-spectrum version. We further consider a 200-class subset of ImageNet-1K which is still relatively large yet requires less compute to experiment with compared to ImageNet-

Table 4: Detection AUROC of post-hoc methods on ImageNet-1K with either the full OOD dataset or the small “clean” version verified by [68]. The numbers in the header are the number of samples in the corresponding dataset.

	Species			SSB-hard			iNaturalist			Places			Textures			OpenImage-O		
	Full 10000	Clean 172	Δ	Full 49000	Clean 208	Δ	Full 10000	Clean 383	Δ	Full 10000	Clean 153	Δ	Full 5160	Clean 288	Δ	Full 15869	Clean 368	Δ
OpenMax [2] (CVPR'16)	71.54	83.09	+11.55	71.37	73.04	+1.67	92.05	92.06	+0.01	82.77	88.99	+6.22	88.10	87.86	-0.24	87.62	87.55	-0.07
MSP [1] (ICLR'17)	75.18	84.43	+9.25	72.09	75.62	+3.53	88.41	88.75	+0.34	80.55	86.00	+5.45	82.43	82.83	+0.40	84.86	84.08	-0.78
TempScale [44] (ICML'17)	75.78	85.58	+9.80	72.87	75.95	+3.08	90.50	90.76	+0.26	82.19	87.95	+5.76	84.95	85.03	+0.08	87.22	86.71	-0.51
ODIN [5] (ICLR'18)	71.68	82.73	+11.05	71.74	71.99	+0.25	91.17	90.90	-0.27	84.47	90.43	+5.96	89.00	88.33	-0.67	88.23	87.95	-0.28
MDS [31] (NeurIPS'18)	58.08	63.66	+5.58	48.50	51.39	+2.89	63.67	64.15	+0.48	51.64	53.88	+2.24	89.80	90.33	+0.53	69.27	71.66	+2.39
MDSEns [31] (NeurIPS'18)	52.27	59.41	+7.14	43.92	47.35	+3.43	61.82	61.67	-0.15	42.23	45.42	+3.19	79.94	79.94	-0.00	60.80	62.52	+1.72
RMDS [45] (arXiv'21)	78.22	86.82	+8.60	71.77	77.18	+5.41	87.24	86.84	-0.40	73.27	80.05	+6.78	86.08	87.62	+1.54	85.84	85.76	-0.08
Gram [46] (ICML'20)	62.55	66.63	+4.08	57.39	56.81	-0.58	76.67	77.19	+0.52	65.27	68.62	+3.35	88.02	87.65	-0.37	74.43	73.87	-0.56
EBO [47] (NeurIPS'20)	71.98	83.08	+11.10	72.08	72.20	+0.12	90.63	90.72	+0.09	83.97	90.06	+6.09	88.70	88.31	-0.39	89.06	88.69	-0.37
GradNorm [48] (NeurIPS'21)	75.79	82.51	+6.72	71.90	68.16	-3.74	93.89	93.74	-0.15	86.05	89.33	+3.28	92.05	91.69	-0.36	84.82	84.00	-0.82
ReAct [13] (NeurIPS'21)	77.63	87.56	+9.93	73.03	74.42	+1.39	96.34	96.44	+0.10	90.93	95.32	+4.39	92.79	92.66	-0.13	91.87	91.72	-0.15
MLS [14] (ICML'22)	72.84	83.86	+11.02	72.51	72.96	+0.45	91.17	91.37	+0.20	84.05	90.10	+6.05	88.39	88.14	-0.25	89.17	88.77	-0.40
KLM [14] (CVPR'22)	74.63	86.36	+11.73	71.38	76.25	+4.87	90.78	91.11	+0.33	79.19	86.16	+6.97	84.72	85.84	+1.12	87.30	86.70	-0.60
VIM [15] (CVPR'22)	68.75	80.51	+11.76	65.54	65.80	+0.26	89.56	90.01	+0.45	79.94	85.66	+5.72	97.97	97.97	-0.00	90.50	91.36	+0.86
KNN [16] (ICML'22)	74.27	83.61	+9.34	62.57	62.71	+0.14	86.41	85.99	-0.42	77.50	84.25	+6.75	97.09	98.06	+0.97	87.04	88.23	+1.19
DICE [49] (ECCV'22)	71.25	82.07	+10.82	70.13	67.87	-2.26	92.54	92.39	-0.15	85.51	90.21	+4.70	92.04	91.42	-0.62	88.26	88.10	-0.16
RankFeat [50] (NeurIPS'22)	36.12	38.89	+2.77	55.89	53.85	-2.04	40.06	39.32	-0.74	65.68	68.58	+2.90	70.90	72.41	+1.51	50.83	50.07	-0.76
ASH [17] (ICLR'23)	79.53	88.44	+8.91	72.89	71.69	-1.20	97.07	97.26	+0.19	90.48	93.97	+3.49	96.90	96.88	-0.02	93.26	93.19	-0.07
SHE [18] (ICLR'23)	75.93	84.10	+8.17	71.08	68.94	-2.14	92.65	92.57	-0.08	87.21	90.34	+3.13	93.60	92.88	-0.72	86.52	85.90	-0.62

Table 5: Detection AUROC of post-hoc methods on ImageNet-200 with either the full OOD dataset or the small “clean” version verified by [68]. The numbers in the header are the number of samples in the corresponding dataset.

	Species			SSB-hard			iNaturalist			Places			Textures			OpenImage-O		
	Full 10000	Clean 172	Δ	Full 49000	Clean 208	Δ	Full 10000	Clean 383	Δ	Full 10000	Clean 153	Δ	Full 5160	Clean 288	Δ	Full 15869	Clean 368	Δ
OpenMax [2] (CVPR'16)	80.76	87.22	+6.46	77.53	79.12	+1.59	92.32	92.52	+0.20	90.73	92.30	+1.57	90.21	91.18	+0.97	88.07	88.54	+0.47
MSP [1] (ICLR'17)	81.81	90.08	+8.27	80.38	82.06	+1.68	92.80	92.89	+0.09	89.38	91.60	+2.22	88.36	89.39	+1.03	89.24	90.12	+0.88
TempScale [44] (ICML'17)	82.24	90.42	+8.18	80.71	82.42	+1.71	93.39	93.48	+0.09	90.16	92.37	+2.21	89.24	90.38	+1.14	89.84	90.65	+0.81
ODIN [5] (ICLR'18)	79.50	89.36	+9.86	77.19	77.77	+0.58	94.37	94.67	+0.30	90.28	93.33	+3.05	90.65	91.88	+1.23	90.11	91.13	+1.02
MDS [31] (NeurIPS'18)	69.53	71.82	+2.29	58.38	58.32	-0.06	75.03	75.18	+0.15	69.80	72.17	+2.37	79.25	80.48	+1.23	69.87	69.85	-0.02
MDSEns [31] (NeurIPS'18)	53.45	59.47	+6.02	50.46	51.57	+1.11	62.16	62.08	-0.08	48.14	50.38	+2.24	80.70	79.73	-0.97	64.96	66.27	+1.31
RMDS [45] (arXiv'21)	84.14	88.96	+4.82	80.20	82.43	+2.23	90.64	90.87	+0.23	89.68	91.72	+2.04	86.77	87.92	+1.15	86.77	87.15	+0.38
Gram [46] (ICML'20)	62.04	61.99	-0.05	65.95	66.79	+0.84	65.30	64.79	-0.51	76.09	74.68	-1.41	80.53	79.14	-1.39	67.72	68.57	+0.85
EBO [47] (NeurIPS'20)	81.33	88.80	+7.47	79.83	81.40	+1.57	92.55	92.63	+0.08	90.37	92.34	+1.97	90.79	91.97	+1.18	89.23	90.04	+0.81
GradNorm [48] (NeurIPS'21)	68.10	79.01	+10.91	72.12	74.43	+2.31	86.06	86.64	+0.58	80.98	84.67	+3.69	86.07	86.95	+0.88	80.66	82.31	+1.65
ReAct [13] (NeurIPS'21)	81.04	88.77	+7.73	78.97	80.78	+1.81	93.65	93.91	+0.26	91.85	93.75	+1.90	92.86	93.58	+0.72	90.40	91.19	+0.79
MLS [14] (ICML'22)	81.74	89.39	+7.65	80.15	81.72	+1.57	93.12	93.18	+0.06	90.67	92.73	+2.06	90.60	91.76	+1.16	89.62	90.40	+0.78
KLM [14] (CVPR'22)	80.47	88.49	+8.02	77.56	78.68	+1.12	91.80	92.19	+0.39	87.49	90.07	+2.58	86.13	87.11	+0.98	87.66	88.70	+1.04
VIM [15] (CVPR'22)	81.99	87.30	+5.31	74.04	74.28	+0.24	90.96	91.04	+0.08	86.88	88.80	+1.92	94.61	95.47	+0.86	88.20	88.75	+0.55
KNN [16] (ICML'22)	85.56	90.74	+5.18	77.03	78.13	+1.10	93.99	94.07	+0.08	87.67	89.60	+1.93	95.29	96.65	+1.36	90.19	91.05	+0.86
DICE [49] (ECCV'22)	80.19	87.51	+7.32	79.06	80.71	+1.65	91.81	91.96	+0.15	88.97	91.06	+2.09	91.53	92.75	+1.22	89.06	90.10	+1.04
RankFeat [50] (NeurIPS'22)	50.10	42.29	-7.81	58.74	57.99	-0.75	33.08	32.40	-0.68	47.10	46.37	-0.73	29.10	26.71	-2.39	52.48	51.97	-0.51
ASH [17] (ICLR'23)	80.70	89.68	+8.98	79.52	81.91	+2.39	95.10	95.28	+0.18	90.80	93.69	+2.89	94.77	95.60	+0.83	91.82	92.79	+0.97
SHE [18] (ICLR'23)	78.61	86.80	+8.19	78.30	80.50	+2.20	91.43	91.68	+0.25	85.99	89.10	+3.11	90.51	91.55	+1.04	87.49	88.69	+1.20

1K. ImageNet-200 has the same 200 categories as ImageNet-R [21]. It shares the same OOD datasets as our ImageNet-1K benchmark. Note that in Table 5 we have similar observations on the effects of dataset noise [68], once again justifying our choice of the selected OOD datasets. In the full-spectrum setting, we again incorporate ImageNet-C, ImageNet-R, and ImageNet-V2.

OOD training data. Our benchmark also specifies OOD training samples $D_{\text{OOD}}^{\text{train}}$ which can be incorporated into training when applicable [27, 28, 29, 30]. To construct $D_{\text{OOD}}^{\text{train}}$ for CIFAR-10/100, we start from the 800 categories in ImageNet-1K that are apart from the 200 classes of TIN and filter out 203 categories relevant to CIFAR-10/100 based on WordNet [71]. Named as TIN-597, the resulting dataset has 597 classes which do not overlap with any of the categories from $D_{\text{OOD}}^{\text{test}}$ and serves as a good candidate for $D_{\text{OOD}}^{\text{train}}$. For ImageNet-200, we directly take the rest 800 categories' images from ImageNet-1K as $D_{\text{OOD}}^{\text{train}}$. We do not consider $D_{\text{OOD}}^{\text{train}}$ for ImageNet-1K since it is hard to find images that do not overlap with $D_{\text{OOD}}^{\text{test}}$, and no relevant methods have considered ImageNet-1K.

B Supported Methods

We briefly overview the supported methods of OpenOOD v1.5. Like in v1 we prioritize methods that have public implementations.

Post-Hoc Inference Methods. Given an input image, OOD detectors often function by assigning an “OOD score” that is computed based on certain outputs from the base classifier, which will then be thresholded to give the binary prediction. The first line of works focus on designing such post-

processors/scoring mechanisms that best separate ID and OOD samples. **MSP** [1] takes the maximum softmax probability over ID categories as the score. **OpenMax** [2] is a replacement for the softmax layer which directly estimates the probability of an input being from an unknown class. **TempScale** [44] calibrates softmax probabilities with temperature scaling. **ODIN** [5] further introduces input preprocessing on top of TempScale. **MDS** [31] fits class-conditional Gaussian distribution on the penultimate layer features of the classifier and derives OOD score with Mahalanobis distance. **MDSEns** [31] is another version of MDS which leverages multiple intermediate layers and forms a feature ensemble. **RMDS** [45] improves MDS by considering the “background score” computed from an unconditional Gaussian distribution. **Gram** [46] identifies abnormal patterns from the Gram Matrices of intermediate feature maps. **EBO** [47] applies energy function to the logits to compute OOD score. **OpenGAN** [6] trains a GAN in the classifier’s feature space and uses the discriminator as the post-processor. **GradNorm** [56] computes the KL divergence between the softmax probability distribution and the uniform distribution and takes the gradients of penultimate layer weights w.r.t. the KL divergence as OOD score. **ReAct** [13] rectifies feature vectors by thresholding their elements with a certain magnitude. **MLS** [14] uses the maximum logit. **KLM** [14] looks at the KL divergence between the softmax probability distribution and a “template” distribution. **VIM** [15] augments the logits with the norm of feature residual compared with ID training samples’ features to compute the OOD score. **KNN** [16] applies KNN to the penultimate layer’s features. **DICE** [49] sparsifies the last linear layer before computing the logits. **RankFeat** [50] transforms the feature matrices such that their rank is 1. **ASH** [17] shapes later layer activations by removing a large portion of the elements and simplifying the rest. **SHE** [18] maintains a template representation for each ID category and detects OOD samples by measuring the distance between the representation of an input to that template.

Training methods without outlier data. Unlike post-hoc methods that only interfere with the inference process, training methods involve training-time regularization to enhance OOD detection capability. **ConfBranch** [51] trains another branch in addition to the classification one to explicitly learn the estimate of model uncertainty. **RotPred** [52] includes an extra head to predict the rotation angle of rotated inputs in a self-supervised manner, and the rotation head together with the classification head is used for OOD detection. **G-ODIN** [32] utilizes a dividend/divisor structure and decomposes the softmax confidence for better ID-OOD separation. **CSI** [7] explores self-supervised contrastive learning objectives for OOD detectors. **ARPL** [53] introduces “reciprocal points” for each ID category and trains the model by pushing the reciprocal point away from the corresponding ID cluster and encouraging OOD samples to gather around the reciprocal point. **MOS** [54] incorporates a two-level hierarchical classifier and designs an accompanying OOD score to benefit OOD detection especially in large-scale settings. **VOS** [41] regularizes the feature space of the classifier under the assumption that the learned representations follow conditional Gaussian distributions. **Logit-Norm** [55] mitigates the over-confidence issue by training and testing with normalized logit vectors. **CIDER** [43] regularizes the model’s hyperspherical space by increasing inter-class separability and intra-class compactness. **NPOS** [42] is a non-parametric version of VOS which removes the Gaussian assumption and instead adopts KNN to model the feature distribution.

Training methods with outlier data. While most methods consider the standard ID-only training, some works assume the access to auxiliary OOD training samples. **OE** [27] is the seminal work in this thread, which lets the classifier learn OOD detection in a supervised fashion. **MCD** [28] considers an ensemble of multiple classification heads and promotes the disagreement between each head’s prediction on OOD samples. **UDG** [29] proposes a clustering-based method to practically extract OOD samples from a mixed pool of auxiliary data and to improve the learned representation quality with unsupervised learning. **MixOE** [30] performs pixel-level mixing operations between ID and OOD samples and regularizes the model such that the prediction confidence smoothly decays as the input transitions from ID to OOD.

Data augmentations. We consider several data augmentation methods which have demonstrated success for improving the generalization ability of image classifiers. **StyleAugment** [22] applies style transfer to clean images to emphasize the shape bias over the texture bias. **RandAugment** [23] randomly sample the augmentation operation and magnitude to increase the diversity of augmented images. **AugMix** [24] linearly interpolate between the clean and the augmented image to preserve the natural looking/fidelity of training images for better generalization. **DeepAugment** [21] manipulates the low-level statistics of clean images by sending them through image-to-image network and distorting the network’s weights. **PixMix** [25] mixes two images with conical combination to create

various new inputs with similar semantics. **RegMixup** [26] trains the model with both clean images and mixed images obtained from convex combination.

C Related Work

To the best of our knowledge, OpenOOD (especially the v1.5 release) is the only work that comprehensively benchmarks various OOD detection methods on multiple ID-OOD pairs. That said, there are still a few works that relate to OpenOOD in certain aspects.

Tajwar et al. [72] made the observation that “OOD detection methods are inconsistent across datasets” from experiments on 3 small datasets (CIFAR-10, CIFAR-100, and SVHN) with 3 specific post-hoc methods (MSP, ODIN, and MDS). While we draw a similar conclusion of “no single winner” in Section 5, our observation comes from the experimentation with 4 datasets and nearly 40 methods from different categories.

A recent work by Galil et al. [73] proposed a method for constructing OOD detection benchmark and evaluated the performance of 5 post-hoc methods with ImageNet-1K pre-trained models. Specifically, for a specific ImageNet-1K model with a specific post-processor, they consider ImageNet-21K images as OOD and categorizes OOD images into a sequence of difficulty groups based on the OOD score from the post-processor. Correspondingly, their evaluation looks at the OOD detection AUROC across all groups, intending to provide a spectrum of AUROC v.s. difficulty. We see two shortcomings of such practice for constructing a general benchmark. First, their benchmarking process is extremely time-consuming since it needs to iterate through nearly all of the samples in ImageNet-21K, which could be prohibitive even for the most lightweight method considering the compute required by common ImageNet models. Second, the resulting benchmark is diagnostic to both the classifier and the post-processor. For example, the first difficulty group of the benchmark for MSP and that for ASH would *not* contain the same OOD samples, making the comparison ambiguous and much less straightforward. In comparison, our carefully designed benchmarks are *standardized*, *i.e.*, agnostic to classifiers and post-processors. Plus, we consider a wide range of methods beyond a few specific post-hoc approaches.

One work that most closely relates to ours is PyTorch-OOD [74], which is a python library for evaluating OOD detection performance. There are several distinctions that separate OpenOOD from PyTorch-OOD. 1) **Number of supported methods.** PyTorch-OOD implements 19 methods as of May 2023 with the most recent one dating back to 2022, while OpenOOD supports 40 approaches including the most advanced ones published in 2023. 2) **Reliability of evaluation results.** PyTorch-OOD still includes as OOD images the LSUN-R and TIN-R [5] which contain obvious resizing artifacts [7]. It also considers ImageNet-O which is known to cause biased evaluation since it is constructed by adversarially targeting a ResNet-50 model with the MSP detector [73]. Their benchmarking results thus can be problematic and unreliable. 3) **Alignment between the goal reflected by the evaluation and human perception.** PyTorch-OOD’s evaluation setup favors detectors that flag covariate-shifted ID samples (*e.g.*, those from ImageNet-R or ImageNet-C) as OOD. We argue that this does not align with human perception and is not an ideal behavior as thoroughly discussed in Section 2 and Section 5.

Another concurrent work by Bitterwolf et al. [68] put up a noise-free OOD dataset (NINCO) for ImageNet-1K in response to the observed noise that exists in popular OOD datasets. They then evaluate 8 post-hoc methods on NINCO and specifically study the effect of large-scale pre-training. OpenOOD is inherently complementary to the work of [68], as we intend to build a comprehensive benchmark for OOD detection by implementing and evaluating various types of methods (not restricting to post-hoc ones) on multiple datasets including ImageNet-1K. Meanwhile, our investigation on full-spectrum detection and findings regarding data augmentation techniques are unique.